

PACS numbers: 42.55.Px; 42.60.Jf; 42.60.Lh
DOI: 10.1070/QE2008v038n11ABEH013866

Radiation parameters of ridge lasers at high pump currents

D.R. Miftakhutdinov, I.V. Akimova, A.P. Bogatov, T.I. Gushchik,
A.E. Drakin, N.V. D'yachkov, V.V. Popovichev, A.P. Nekrasov

***Abstract*. Quantum-well ridge GaAs/AlGaAs heterostructure lasers are studied at high pump currents. It is shown that their catastrophic optical damage (COD) is preceded, as a rule, by a giant kink caused by the collapse of a waveguide in a horizontal plane. It is found that, by increasing the coating thickness of the output end-face of a diode by preparing an intermediate ZnSe layer between the cleaved output end-face of the diode and a coating forming the output mirror of the laser, it is possible to increase the COD threshold by a factor of 1.5 – 2. This optical strengthening occurs because the ZnSe layer provides an additional channel for heat sink from the overheated output face.**

Keywords: *high-power semiconductor laser, catastrophic optical degradation, optical damage of the output face.*

1. Introduction

Increasing the output power of semiconductor lasers is still one the most important problems. In particular, this problem for near-IR lasers (0.8 – 1.2 μm) is directly related to the enhancement of the radiation resistance of the output face. Indeed, at optical flux densities $\sim 10^7$ W cm^{-2}, the so-called catastrophic optical degradation (COD) of a laser appears, which is manifested, as a rule, in the optical damage of the output face of the diode [1 – 3]. This degradation restricts the output power W of the laser and the optical beam brightness [4] (if the laser operates in the transverse single-mode regime). Despite a great number of theoretical papers devoted to the COD problem (see, for example, [5 – 7] and references therein), this process has not been comprehensively investigated so far. The problem of improving the radiation resistance of the output mirror still remains urgent. In this connection it is interesting to study the COD dynamics for lasers with output faces with different coatings.

D.R. Miftakhutdinov, I.V. Akimova, A.P. Bogatov, T.I. Gushchik, A.E. Drakin, N.V. D'yachkov P.N. Lebedev Physics Institute, Russian Academy of Sciences, Leninsky prosp. 53, 119991 Moscow, Russia; e-mail: bogatov@sci.lebedev.ru;
V.V. Popovichev, A.P. Nekrasov M.F. Stel'makh Polyus Research & Development Institute, ul. Vvedenskogo 3, 117342 Moscow, Russia

Received 8 April 2008
Kvantovaya Elektronika **38** (11) 993 – 1000 (2008)
Translated by M.N. Sapozhnikov

In addition, the study of the behaviour of semiconductor lasers at very high pumping levels is of interest in itself because during the propagation of an intense optical beam in the resonator, the laser operates in the deep saturation regime. Usually, this behaviour escapes researchers because the COD onset excludes the possibility of performing experiments in cw or repetitively pulsed regimes. The recording of emission parameters before the COD onset used in our study eliminates this restriction, allowing us to obtain new data on the interaction of the intense laser beam with an amplifying active region.

We investigated quantum-well ridge lasers operating upon moderate pumping in the transverse single-mode regime. Such lasers were chosen to provide 'purest' measurements of the COD threshold. Unlike lasers with a wide active region ($\sim$ 100 μm and more), the optical flux density in a transverse single-mode laser can be estimated quite accurately. The transverse radiation intensity distribution along the active-layer plane in lasers with a wide active region is strongly nonuniform due to filamentation [8] and the local radiation intensity can exceed the average value by an order of magnitude. In addition, this transverse intensity distribution can vary in time at the nanosecond and subnanosecond scales, so that the intensity distribution 'averaged' in time and over the active-region width strongly differs from the intensity distribution at which the COD occurs.

2. Experimental

The composition and thickness of AlGaAs/GaAs heterostructure layers used in ridge lasers studied in the paper are presented in Table 1. All the lasers had resonators with almost identical parameters: the ridge structure optimised by the method used in [4], the length of 1 mm, and the coating of the rear face with the reflectivity $\sim$ 95 %. The coatings of the output faces of the lasers were different.

Table 1. Parameters of the AlGaAs/GaAs heterostructure layers.

Composition	x, y	Layer thickness/μm	Refractive index
P^+-GaAs	–	0.35	3.6436
P-$Al_yGa_{1-y}As$	0.37	1.95	3.3557
$Al_xGa_{1-x}As$	0.31	0.12	3.3956
GaAs	–	0.009	3.6436
$Al_xGa_{1-x}As$	0.31	0.12	3.3956
N-$Al_yGa_{1-y}As$	0.37	2.74	3.3557
n-GaAs	–	100	3.529

Depending on this coating, the lasers were divided into four groups (Table 2). Samples of group A had no special coating and their output face was a simple cleavage. The output faces of group B samples had AR coatings. The faces of samples of groups C and D were coated with a ZnSe layer immediately after cleavage; in addition, AR coatings were deposited on the faces of group D samples.

Table 2. Coating of the output faces of samples.

Group	Presence of a ZnSe layer of thickness $d = \lambda/2$	AR coating
A	absent	absent
B	absent	$R \approx 7\,\%$
C	present	absent
D	present	$R \approx 5\,\%$

Note: R is the reflection coefficient.

Due to the inevitability and irreversibility of the COD process at high pumping levels, we first measured the watt–ampere characteristics, spectra, and radiation patterns at moderate pump currents.

Studies were performed in two regimes by using quasi-continuous or pulsed pump currents. The experimental setup is described in [1]. Radiation from a laser diode was focused by means of an objective on a fast LFD-3 avalanche photodiode, whose output signal was fed to one of the two channels of a storage Tektronix TDS-2022 oscilloscope. A signal proportional to the pump current was fed to another channel. Both signals were processed in a PC connected with the oscilloscope.

A power supply of lasers studied by using the quasi-continuous pump current was a generator of single saw-tooth pulses with the ~ 6-μs rise time and the current amplitude ~ 4 A, which resulted, as a rule, in the optical breakdown of a laser diode. The current rise time was chosen to provide the maximum possible time resolution (2 ns per count) of the oscilloscope used in experiments. The preliminary study of the time response of the detection circuit (photodiode-cable) with the help of an S-91 stroboscopic oscilloscope showed that this time is adequate to the sampling frequency used in experiments. The pulsed pump current was provided by a rectangular pulse generator producing individual 50–200-ns pulses or generated at a repetition rate of 1 kHz.

3. Basic emission characteristics of samples

Figure 1a presents typical watt–ampere characteristics of laser diodes from each of the groups measured with an FD-24 photodiode on the automated setup. Power calibration was performed by means of an Ophir 12V-A1 power meter. These watt–ampere characteristics were then used for power calibration in measurements at high pump currents.

Typical emission spectra of lasers studied in our experiments consist of a few tens of longitudinal modes with an irregular envelope, as shown in Fig. 1b for the spectra of one of the samples from group D. The red shift of the envelope with increasing the pump current is caused by the heating of the sample by $\sim 10\,^{\circ}$C, according to the estimate.

The radiation pattern in the vertical plane shown in Fig. 2a is determined by the composition of heterostructure layers, which have considerably different refractive indices (the difference achieves a few tenths of unity), and therefore

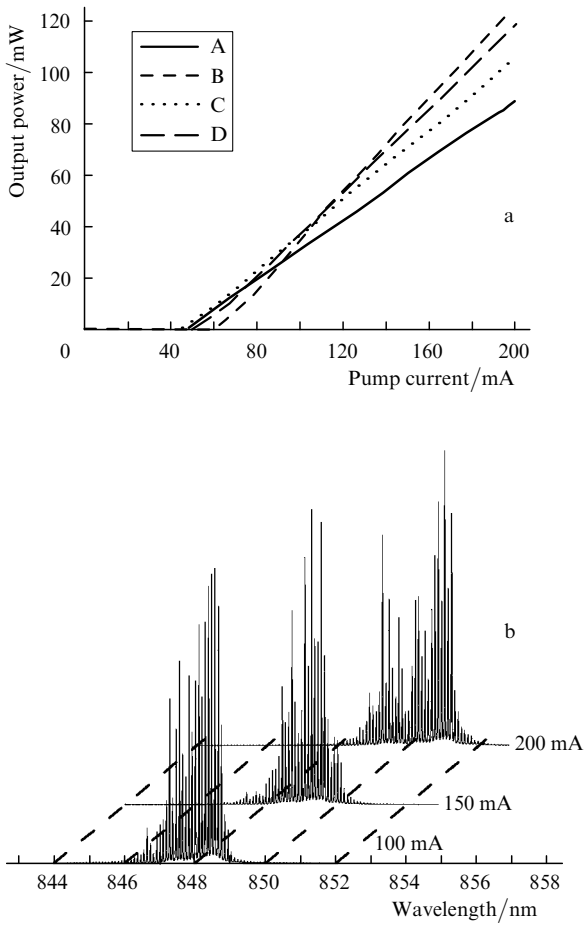

Figure 1. Watt–ampere characteristics of samples from groups A–D (a) and typical emission spectra of a sample of group D (b) at moderate pump currents.

is independent of the pump current, the presence of the reflecting or AR coatings of diode faces, etc. One can see that, when the pump current is changed approximately from $2J_{\rm th}$ to $4J_{\rm th}$, the radiation pattern changes insignificantly, the intensity of its wings increasing only by $\sim 1\,\%$ of the total radiation energy.

Unlike the radiation pattern in the vertical plane, the radiation pattern in the horizontal plane (Fig. 2b) depends on the pump current and also changes from sample to sample. This is explained by the fact that the built-in difference in the effective refractive indices along the horizontal direction amounts to a few thousandths of unity and is of the order of magnitude of the characteristic change in the refractive index with temperature or the concentration of carriers. Such a behaviour of the horizontal radiation pattern is caused both by the structure of the optical waveguide in each particular sample and by the dynamic change of its parameters during the spatial burning out of inversion. This circumstance is studied in more detail in [9]. However, Fig. 2b shows that the radiation pattern changes weakly at moderate pump currents: in fact, only the position of its maximum changes, whereas the width remains almost constant. In this case, we can assume that the transverse intensity distribution of an optical beam at the output mirror will change not very strongly, at least, for estimating the beam cross section and the radiation power density.

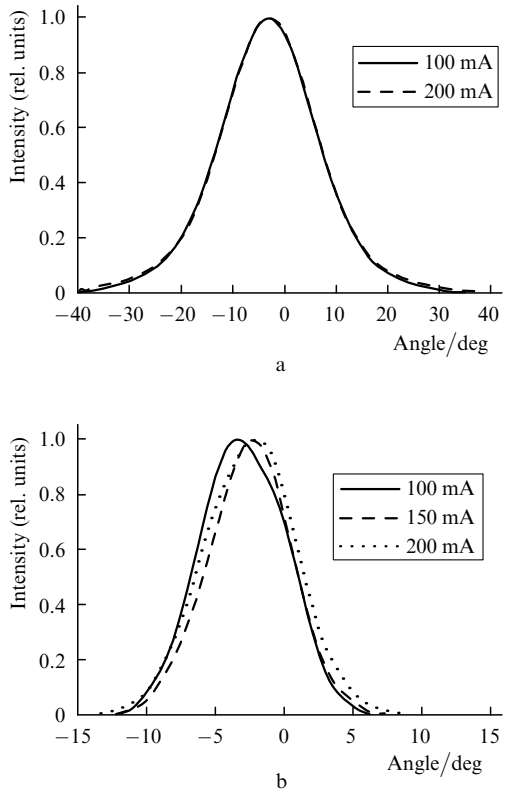

Figure 2. Typical radiation patterns of samples at moderate pump powers in a plane perpendicular to layers (a) and in a horizontal plane (b).

4. Results

Figure 3 presents the time dependences of the output optical power in the case of saw-tooth pump current pulses, i.e. in the quasi-continuous regime. Typical curves are shown for lasers from each of the groups, which characterise their behaviour at limiting output powers up to the COD. In some sense, these are watt – ampere characteristics presented in the implicit form as parametrically specified time dependences of the optical power and pump current. Because the time dependence of the pump current is virtually linear (possibly, except a small interval discussed below), the power curve can be treated as the watt – ampere characteristic.

The drastic decrease in the output power of lasers is caused by the COD, which leads, as a rule, to the optical damage of the output face of the laser diode (microphotographs of the damaged output faces of samples from groups A, B, C, and D are presented in Fig. 4).

The time dependences of the output power presented in Fig. 3 are qualitatively similar for all groups of samples. However, certain quantitative differences are observed. Consider these differences in more detail for dependences $P_{\text{out}}(t)$.

Figure 5 shows in detail the time dependence of the output power at the high pump level for one of the lasers of group B. As the pump current is increased, the output power first increases almost linearly, then the slope efficiency decreases and the output power achieves its maximum value $P_{\max}$. Thereafter the output power decreases, achieves a

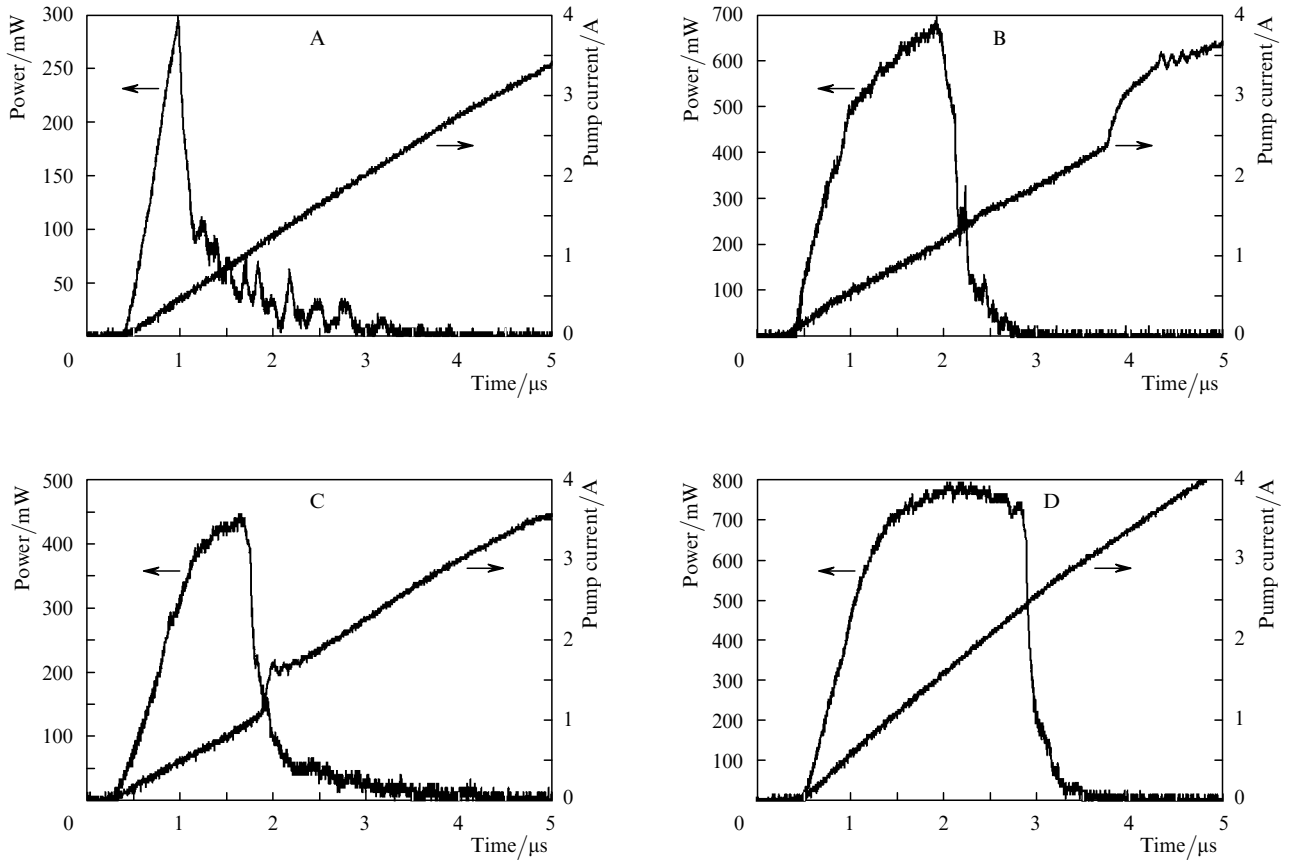

Figure 3. Time dependences of the pump current and output power at high pump levels for samples of groups A, B, C, and D.

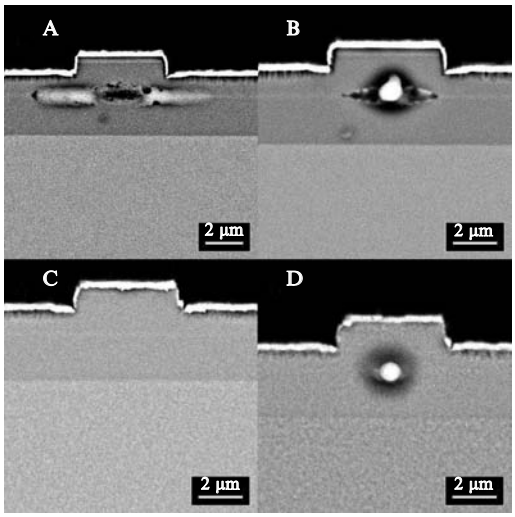

Figure 4. Microphotographs of the output faces of samples from groups A, B, C, and D after the COD.

critical value P_{cr} and drastically, for a few tens of nanoseconds, decreases down to the intermediate level P_{int}, which is several times lower than the maximum level. And, finally, the output power decreases for several hundreds nanoseconds to the spontaneous emission level.

Within the time $\Delta t \approx 1.6$ μs after the optical damage of the output face of the sample, a jump in the pump current occurs. It is within this short interval of duration of about 100 ns that the time dependence of the pump current differs from a linear dependence, as mentioned above. The power supply of the laser is a voltage source loaded by the laser and a ballast resistance connected in series. Therefore, the pump current jump can be caused by a decrease in the diode resistance. During repeated pump pulses, the time dependence of the pump current acquires a new slope, which indicates that a current channel shunting the diode is irreversibly formed. It seems that this shunting channel is a short circuit formed by the local region of optical damage of the face enriched with metal elements of the third group.

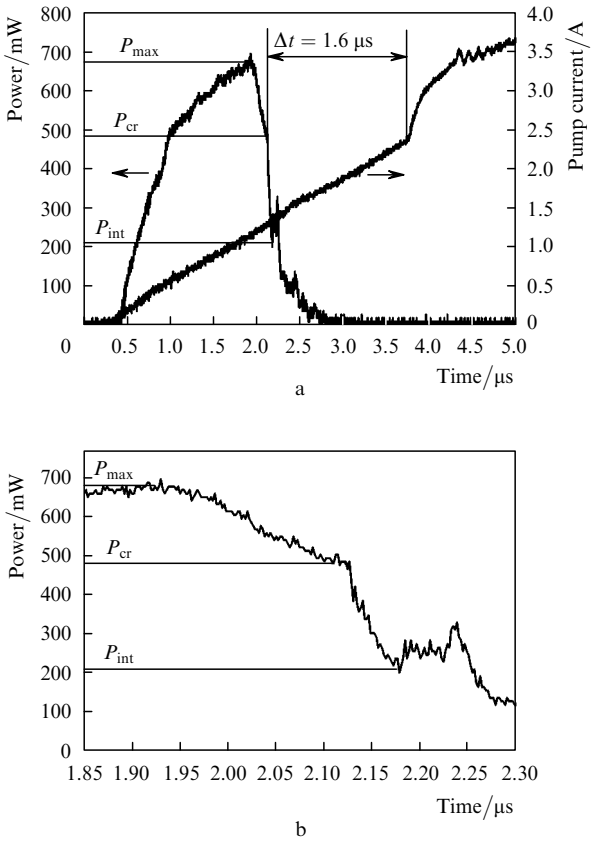

Figure 5. Time dependences of the pump current and output power at high pump levels for a sample of group B (a); the same time dependence of the output power at the enlarged time scale.

Note that the short circuit appears in the given case within ~ 1.6 μs after the optical damage onset. The delay time for other samples varied almost from zero to the pulse end time. For some samples, shunting channels did not appear at all.

Consider now in more detail the behaviour of different samples in the quasi-continuous pumping regime. A characteristic feature of the samples of group A is their linear or almost linear watt – ampere characteristic (without kinks) up to the damage of the output face (Fig. 3a). The damage threshold P_{cr} for this laser was ~ 300 mW. Figure 4a presents the electron-microscope photograph of this sample after its damage. On the output face under the ridge an almond-shaped damage region is observed. A similar optical breakdown picture was described earlier in paper [1].

Unlike samples of group A, the samples of other groups have strongly nonlinear watt – ampere characteristics at high output powers (Figs 4b – d). However, this nonlinearity appears at powers exceeding 400 – 500 mW, and therefore the absence of a kink for samples of group A is explained by the fact that they experience the COD before the kink appearance. Kinks are most strongly manifested for samples of group D, which have the thickest coating of the output face among all the lasers studied. A specific feature of lasers of this group is a very long steep slope of the watt – ampere characteristic, which continues until the damage of the output face. Figure 6 shows the development of degradation for a sample with the longest duration of such a steep slope. One can see that during ~ 2 μs, when the pump current increases almost up to 2.5 A, the output power almost does not change. For other samples of this group, the characteristic steep slope time is about 1.5 μs, which is also much longer than that for samples of other groups. In addition, the damage of faces of samples of group D occurs for a considerably longer time compared to samples of other groups. Indeed, the output power decreases quasi-monotonically during ~ 300 ns.

The damage pattern of output faces for diodes from groups B – D (Figs 4b – d) also differs from that for samples from group A. Damage regions shown in Figs 4b and d are considerably smaller and are nearly circular. Figure 4c demonstrates a particular case when no visible damage of the face was observed. Nevertheless, the watt – ampere characteristic of this sample indicates that it also was subjected to the COD. Note that the absence of the visible damage of the output face of this diode is not typical for samples of group C. The damage pattern for most of the samples of this group was similar to that presented in Figs 4b and d. In rare cases samples of groups B and D also did not reveal any visible damage.

Samples of group A never revealed the absence of the visible damage of faces caused by the COD, which is

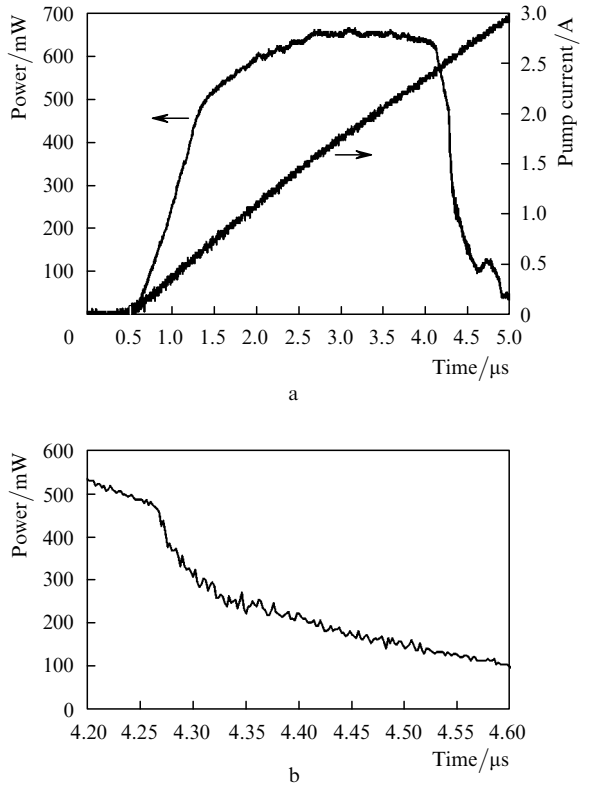

Figure 6. Time dependences of the pump current and output power at a high pump level for a sample of group D (a); the same time dependence of the output power at the enlarged time scale (b).

although a rare but general property of lasers with output faces covered with coatings. Our investigations showed the damage is produced in samples for which P_{cr} is considerably lower for some reason than its typical value for the given group. For example, the typical value of P_{cr} for group B is ~ 540 mW, whereas $P_{cr} \approx 390$ mV for a sample in Fig. 4c.

The power characteristics of lasers pumped by a quasi-continuous current are presented in Table 3, where, apart from output powers, the total internal power of the incident and reflected waves near the output mirror upon COD is also indicated.

Table 3. Critical powers of lasers of groups A – D.

Group	P_{max}/mW	P_{cr}/mW	P_{in}/mW	$S_{CD}/10^7$ W cm^{-2}
A	300	300	557	4.64
B	670	470	530	4.42
C	540	540	1000	8.33
D	750	650	732	6.10

Note: P_{max} is the maximum achieved power; P_{cr} is the critical power level; P_{in} is the total intracavity power near the output mirror; S_{CD} is the COD power density.

Below, we present the results obtained upon pulsed pumping. Figure 7a shows typical pump current and output power pulses of a laser. Our current source cannot produce a strictly rectangular pump pulse, and therefore the value of the pump current will be defined below as the current averaged over a pulse. The watt – ampere characteristic in the case of 100-ns pump pulses is shown in Fig. 7b. One can see that the output power at currents exceeding 6 A ceases to grow and even slightly decreases. The tendency of the dynamic watt – ampere characteristic to saturate and even to acquire the negative slope can be observed by comparing the shapes of current and radiation pulses (Fig. 7a). Indeed, the top of the current pulse has the positive slope, whereas the radiation pulse in this time interval has the negative slope.

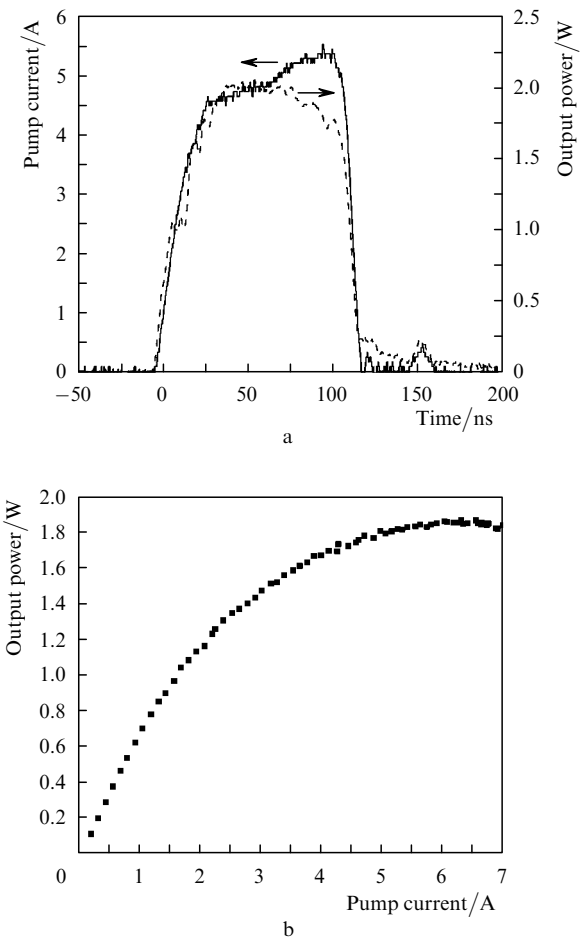

Figure 7. Pump current and radiation power pulses (a) and the watt – ampere characteristic in the pulsed regime (b).

The watt – ampere characteristic in the pulsed regime (Fig. 7b) differs from that in the quasi-continuous regime (Fig. 3) by the absence of a drastic decrease in the output power caused by the COD during the first pump pulse only. Of course, such degradation takes place upon pulsed excitation as well; however, its reliable detection proved to be complicated, at least, for pump pulses of duration exceeding 100 ns. It seems that in this case defects are produced after several pulses. As a result, the output power changes strongly not during the first pump pulse but after many radiation pulses. Such degradation occurred in our experiments at pulsed powers $\sim 1.7 - 1.8$ W, which is close to the power level corresponding to the saturation of the watt – ampere characteristic (Fig. 7b).

To elucidate the reason for the output power saturation with increasing pump current, we recorded emission spectra at pump pulses of different durations (Fig. 8). One can see that the emission spectrum has a complex shape even at the pulse duration of ~ 30 ns. A great number (more than a hundred) of longitudinal modes covering the spectral range of width ~ 13 nm are excited. The modes are observed quite

distinctly, which means the absence of chirping, which could smooth out the spectrum. However, as the pump pulse duration is increased up to 50 ns and then to 100 ns, the smoothing of the modes appears and increases. And although the spectral peaks corresponding to longitudinal modes are still observed, their contrast considerably decreases. This means that the dynamic change of the optical length of the resonator during the pulse due to a change in the effective refractive index becomes already comparable with half the wavelength. Another specific feature of the emission spectrum at high excitation levels is that the spectrum envelope has a complex shape, containing two – three local maxima. Note that, although the intensity of these maxima changes and their width increases, their spectral position change only weakly with increasing pump pulsed duration. This means that the influence of the active-medium heating on the gain band during a pump pulse is insignificant.

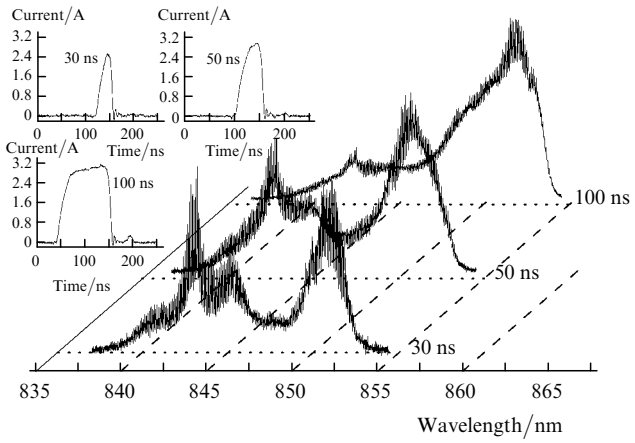

Figure 8. Emission spectra in the pulsed regime at pump pulses of different durations.

Figure 9 shows the dependence of the radiation pattern in the horizontal plane on the pump current in the pulsed regime. As the pump current is increased, the radiation pattern broadens and exhibits noise. The noise appears because the radiation pattern is recorded not per pulse but during many pulses, each of them having its own radiation pattern. In the case of limiting pump currents, the width of the time-averaged radiation pattern increases more than twice. Obviously, this is also explained by the change of the radiation pattern during the pump pulse.

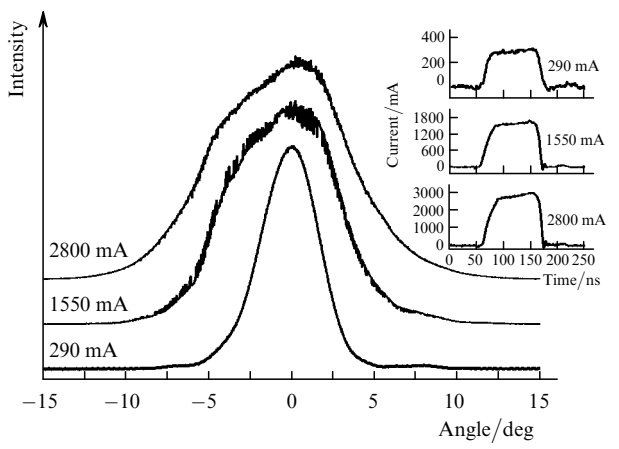

Figure 9. Radiation patterns in a horizontal plane in the pulsed regime for different pump currents.

5. Discussion of results

The experimental results presented above demonstrate two important effects inherent in lasers at high excitation levels. The first effect is the saturation of the watt – ampere characteristic and even its decrease (negative slope) beginning from certain current levels. Note that this takes place even in the dynamic regime, when the overheating of the active region, at least 'averaged' over the resonator length, is excluded.

The saturation of the watt – ampere characteristic and its declining part can be called a giant kink (similarly to analogous by weaker anomalies of watt – ampere characteristics at moderate pump levels). Our experimental data suggest that this giant kink appears due to a considerable deterioration of the waveguide properties of the laser resonator in the plane of structure layers (collapse of a horizontal waveguide) caused by the antiwaveguide action of carriers injected into the active region. While the antiwaveguide action of carriers at moderate pump currents (100 – 200 mA) only weakens a 'built-in' waveguide produced due to the ridge geometry of a diode, at pump currents ~ 2 A the antiwaveguide action of carriers is so strong that it 'ejects' an optical beam from a pumped region. The spatial overlap of the region filled by the optical flux and of the gain region drastically decreases, resulting in the power saturation or even decrease. The 'ejection' of the field is characterised by the instability because the spatially inhomogeneous burning out of inversion (due to stimulated transitions) leads to the self-action of the optical beam on its propagation geometry in the resonator. At moderate excitation levels, these effects were investigated in detail experimentally and theoretically in [9], and here they are represented in Fig. 2b by a variation in the radiation pattern. It is obvious that at an order of magnitude higher pump current these effects are so strong that they change not only the watt – ampere characteristic but the emission spectrum as well. The radical dynamic change in the radiation pattern and the gain spectrum with changing the waveguide properties of the active region was observed long ago (see, for example, [10]) for stripe lasers with a waveguide formed by the gain.

The trajectory of an optical beam in a resonator [9] is a winding curve. Its local deviations from the optical axis of the resonator are comparable with or even exceed the transverse size of the active region. This is confirmed by the broadening of the radiation pattern by more than twice (Fig. 9). In this case, the resulting amplification is formed by spatial regions having different material amplification bands.

Note here that the position of the material amplification band maximum in a semiconductor active medium (this concerns especially quantum-well layers) strongly depends on the carrier concentration. Thus, it follows from experimental data [11] that this maximum shifts by ~ 10 nm with changing the carrier concentration by $\sim 30\,\%$ (from 1.0×10^{18} to 1.3×10^{18} cm^{-3}). The propagation of the beam from one resonator mirror to another is accompanied

by its amplification in spatial regions with spectral maxima displaced with respect to each other. Thus, the resulting amplification band of the optical beam with a winding trajectory can have two or more local maxima.

Because the spatial configuration of the optical beam in the resonator at high pumping levels is principally unstable, it is obvious that the amplification band, the number of local maxima and their widths for a particular laser cannot be simulated. It seems that this problem can be solved only by eliminating the spatial instability of the optical beam, thereby improving its quality.

The second and quite expected effect observed at high pumping levels is the catastrophic degradation of a laser, which is accompanied, as a rule, by the optical damage of the output face of a laser diode. We investigated in this paper the influence of the optical coating of the output face on the type of its damage and found that the radiation resistance of the output face increased with increasing the coating thickness. This is demonstrated by the data presented in Table 3, according to which the radiation resistance of diodes considerably increases when their output faces are coated with a ZnSe film (diodes of groups C and D). This conclusion is not too trivial, taking into account that not the coating itself, which is transparent for laser radiation, is subjected to damage, but the active region and facing layers of the laser diode. Note that data on the optical damage of diode faces without coatings obtained in our paper for the GaAs active region are close to the data obtained in [1] for uncoated InGaAS faces. This means that quantitative parameters of damage processes for GaAs and InGaAs faces are also close.

The fact that the circular damaged region of the coated output face of the laser is considerably smaller than the almond-shaped damaged region of the uncoated output face also suggests that the overheated part of the active region is cooled through the film deposited on the face. It is most likely that the role of the ZnSe film is reduced only to additional heat removal. Although this increases the critical optical damage power P_{cr}, it is unlikely that this film can serve as the efficient passivating coating changing considerably the physical properties of the cleaved face surface. Indeed, if the COD occurred without the optical damage of the output face, the detected power P_{cr} was not higher but lower than its typical value. This means that the face was not damaged not due to increase in its radiation resistance but due to the presence of regions in the active medium with damage thresholds lower than the damage threshold of the output face. Therefore, a search for the technology of manufacturing passivating coatings, which could increase considerably the value of P_{cr}, remains of current interest.

Analysis of the optical damage dynamics suggests that there exists an inertial process of duration ~ 100 ns (or longer) preceding the formation of the irreversible damage of the output face. This is confirmed by the absence of a drastic decrease in the output power during a short (shorter than 100 ns) pump pulse even in the case of a very high pump level (up to 6 A). This inertial process can be the heating of spatial regions in a laser diode which are adjacent to the overheated region and can be subject to melting and optical damage. Note that, according to data obtained in [1] and our study, the process of irreversible damage of an overheated local region on the output face proceeds, as a rule, for 20–40 ns (for example, the time during which power decreases from P_{cr} to P_{int}, Fig. 5b). This time is required only for the accumulation of energy equal to the melting heat in a small volume of the overheated region. This process proceeds at almost constant temperature, which is equal to the melting temperature of the active region material. In this case, the temperature of adjacent regions does not change and energy is not spent in these regions. However, to increase the temperature of a region, which can be potentially subjected to damage, from the working temperature (~ 300 K) to the melting temperature (~ 1500 K), the additional energy is required for heating adjacent regions because temperature gradients cannot be infinitely large. The accumulation of such energy can be the inertial process mentioned above. Therefore, the apparent absence of catastrophic degradation or an increase in its threshold upon pumping the laser by short pulses means only that degradation occurs not during the first pulse, as upon quasi-continuous pumping, but is characterised by a gradual growth of a damaged region from pulse to pulse.

6. Conclusions

The use of additional ZnSe coatings on resonator mirrors provides the increase in the critical damage power by 1.5–2 times. The output-face coatings with the increased thickness and high heat conductivity are promising. In this connection ZnSe is one of the most convenient materials because its lattice constant is close to that of GaAs, which makes it possible to prepare quite thick layers without noticeable defects and microcracks and with good adhesion to the cleaved GaAs surface.

Nevertheless, the development of a passivating coating for further considerable increasing the laser output power is still urgent. In addition, our study has shown that, to increase the output power of a laser in the transverse single-mode regime, it is necessary not only to improve the radiation resistance of the output face but also to develop the horizontal waveguide of the resonator providing operation at high pump currents without the appearance of the giant kink of the watt–ampere characteristic.

Acknowledgements. This work was partially supported by the program 'Quantum Nanostructures' of the Presidium of RAS, the Federal program 'Research and Development in the Priority Directions in the Development of the Scientific and Technological Complex of Russia in 2007–2012' (State Contract No. 02.513.11.3168) and Grant No. NSh-3168.2008.02 of the President of the Russian Federation for the State Support of Leading Scientific Schools.

References

1. Akimova I.V., Bogatov A.P., Drakin A.E., Konyaev V.P. *Kvantovaya Elektron.*, **25**, 647 (1998) [*Quantum Electron.*, **28**, 629 (1998)].
2. Eliseev P.G. *Progr. Quantum Electron.*, **20**, 1 (1996).
3. Walker C.L., Bryce A.C., Marsh J.H. *IEEE Photon. Techn. Lett.*, **14**, 1394 (2002).
4. Popovichev V.V., Davydova E.I., Marmayuk A.A., Simakov A.V., Uspenskii M.B., Chel'nyi A.A., Bogatov A.P., Drakin A.E., Plisyuk S.A., Stratonnikov A.A. *Kvantovaya Elektron.*, **32**, 1099 (2002) [*Quantum Electron.*, **32**, 1099 (2002)].
5. Schatz R., Bethea C.G. *J. Appl. Phys.*, **76**, 2509 (1994).
6. Menzel U. *Semicond. Sci. Techn.*, **13**, 165 (1998).
7. Smith W.R. *J. Appl. Phys.*, **87**, 8276 (2000).

8. Bogatov A.P., Drakin A.E., Stratonnikov A.A., Konyaev V.P. *Kvantovaya Elektron*., **30**, 402 (2000) [*Quantum Electron*., **30**, 402 (2000)].
9. Plisyuk S.A., Batrak D.V., Drakin A.E., Bogatov A.P. *Kvantovaya Elektron*., **36**, 1058 (2006) [*Quantum Electron*., **36**, 1058 (2006)].
10. Alaverdyan S.A., Bazhenov V.Yu., Bogatov A.P., Gurov Yu.V., Eliseev P.G., Okhotnikov O.G., Pak G.T., Rakhval'skii M.P., Khairetdinov K.A. *Kvantovaya Elektron*., **7**, 123 (1980) [*Sov. J. Quantum Electron*., **10**, 68 (1980)].
11. Batrak D.V., Bogatova S.A., Borodaenko A.V., Drakin A.E., Bogatov A.P. *Kvantovaya Elektron*., **35**, 316 (2005) [*Quantum Electron*., **35**, 316 (2005)].